JOURNAL OF CATALYSIS 86, 342–358 (1984)

Chemisorption and Catalysis by Metal Clusters

III. Hydrogenation of Ethene, Carbon Monoxide, and Carbon Dioxide, and Hydrogenolysis of Ethane Catalyzed by Supported Osmium Clusters Derived from $Os_3(CO)_{12}$ and from $Os_6(CO)_{18}$

S. DAVID JACKSON,[1,2] RICHARD B. MOYES, PETER B. WELLS,[2] AND ROBIN WHYMAN*

*Department of Chemistry, The University, Hull, England, HU6 7RX; and *ICI New Science Group, P.O. Box 11, Runcorn, England, WA7 4QE*

Received August 25, 1982; revised July 4, 1983

Properties are described for catalysts containing high nuclearity metal clusters (nuclearity ~12) derived from $Os_3(CO)_{12}$ and $Os_6(CO)_{18}$ and supported on silica, alumina, titania, or ceria. Ethene hydrogenation (325–535 K), ethane hydrogenolysis (395–665 K), CO hydrogenation (455–665 K), and CO_2 hydrogenation (455–715 K) have been examined in pulsed-flow and static reactors. The high nuclearity osmium clusters, protected against sintering by retained ligand-CO, ligand-C, and a support–cluster interaction, are stable under these conditions and provide highly reproducible activity. Freshly prepared catalysts each exhibit an initial non-steady state, during which hydrocarbon is progressively retained and activity rises, passes through a maximum, and declines to a steady state value. Catalysts in the steady state continue to retain hydrocarbon which is probably branched in structure and unsaturated in character. Such retained hydrocarbon species mediate hydrogen atom transfer to reacting adsorbed species. Their concentrations, which have been determined by infrared spectroscopy, ^{14}C-tracer studies, and material balances, are compared with the known site concentrations associated with fresh cluster-derived catalysts. Catalysts in the steady state exhibit activities the magnitudes of which diminish with increasing support–cluster interaction, viz., silica-supported clusters > titania-supported clusters > alumina-supported clusters. Preliminary measurements using a ceria-supported catalyst suggest that activity versus the strength of the support–cluster interaction exhibits a "volcano" relationship. Adsorption of ethene, ethane, and CO occurs at osmium atom sites on the high nuclearity osmium clusters, and the reaction intermediates are also adsorbed at these sites. CO_2, however, is adsorbed and reacts at ligand-C sites. Detailed mechanisms are presented for ethene, CO, and CO_2 hydrogenations, of which some aspects have been investigated by use of ^{14}C as an isotopic tracer. Most cluster-derived catalysts show exceptional activity for ethane hydrogenolysis, some apparent turnover numbers being 2 orders of magnitude higher than for supported metallic osmium. The osmium clusters adsorb reactants less strongly than metallic osmium, because of their commitment to bonding with the protective CO-ligands, and this weaker reactant adsorption may provide superior catalytic properties.

INTRODUCTION

Part I (*1*) described our characterisation of silica-, alumina-, and titania-supported catalysts which contain osmium clusters. These clusters, though derived from $Os_3(CO)_{12}$ or from $Os_6(CO)_{18}$, have high nuclearity (probably ~12) and are stabilised against sintering by the retention of some ligand-CO and by cluster–support interactions. Some chemisorption properties of these materials were described in Part II (*2*), and their catalytic properties are reported here. The hydrogenation and hydrogenolysis activities of these catalysts are not poisoned by their exposure to air at

[1] Present address: ICI New Science Group, P.O. Box 11, Runcorn, England, WA7 4QE.

[2] To whom correspondence should be addressed.

0021-9517/84 $3.00
Copyright © 1984 by Academic Press, Inc.
All rights of reproduction in any form reserved.

room temperature (*3*), which contrasts with the behavior of conventional supported osmium.

EXPERIMENTAL METHODS

Catalyst Preparation and Nomenclature

The preparation and characterisation of the materials employed as catalysts in the present work have been described in Parts I and II (*1, 2*). Briefly, impregnation of $Os_3(CO)_{12}$ or of $Os_6(CO)_{18}$ from nonaqueous solutions onto heat-treated silica, alumina, or titania provides a heterogeneous dispersion of the unchanged cluster compound on the support. Subsequent heating of the freshly impregnated materials in vacuum or in a helium stream to 523 K provides the high nuclearity clusters which we term "species A." These species A have the capacity to chemisorb H_2, O_2, CO, and hydrocarbons, and to catalyze hydrogenations and hydrogenolyses. In Part II, we established that CO adsorbs strongly at sites involving osmium atoms and weakly at sites involving ligand-C. Oxygen, likewise, adsorbs strongly at sites involving osmium, but does not adsorb at sites involving ligand-C. No interconversion of ligand-CO and adsorbed-CO occurs below 523 K.

When we refer to the supported catalysts as materials, we do so by reference to the parent cluster used in the preparation and the support, e.g., $Os_3(CO)_{12}$/silica, $Os_6(CO)_{18}$/alumina, etc. even though the active entities present are the high nuclearity clusters. When we refer to the catalytically active entities themselves, however, we adopt phrases such as "species A derived from $Os_3(CO)_{12}$," etc. The mean empirical compositions were given in Part I as: species A derived from $Os_3(CO)_{12}$/silica, $Os_n(CO)_{2.8n}C_{0.1n}Z_{0.3n}$; species A derived from $Os_3(CO)_{12}$/alumina, $Os_n(CO)_{2.2n}C_{0.1n}Z_{0.15n}$; species A derived from $Os_3(CO)_{12}$/titania, $Os_n(CO)_{2.0n}C_{0.2n}Z_{0.8n}$; species A derived from $Os_6(CO)_{18}$/silica, $Os_n(CO)_{2.8n}C_{0.2n}Z_{0.15n}$; species A derived from $Os_6(CO)_{18}$/alumina, $Os_n(CO)_{2.2n}C_{0.4n}Z_{0.5n}$; species A derived from $Os_6(CO)_{18}$/titania, $Os_n(CO)_{2.0n}C_{0.1n}Z_{0.2n}$; where two Z-entities constitute an adsorption site for one CO molecule or for one O_2 molecule adsorbed in a bridged configuration (*2*), and n has the most likely value of 12.

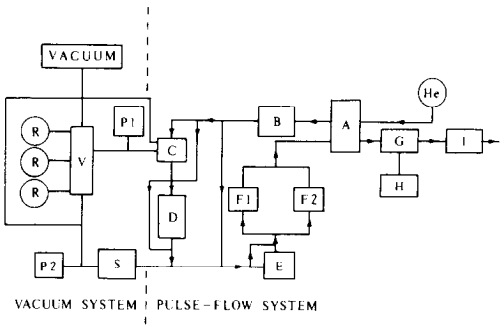

FIG. 1. Schematic representation of the apparatus. The flow system is shown at the right-hand side; arrows indicate the direction of the helium flow. (A) katharometer; (B) input flow meter; (C) standard volume; (D) pulsed-flow reactor; (E) trap; (F1, F2) GLC columns; (G) Geiger–Müller counter; (H) scalar-rate meter; (I) output flow meter. Reactants stored in vessels R were mixed in volume V before being metered either into C for transmission to the flow reactor or into the static reactor S. (P1, P2) Pressure transducers.

Apparatus and Materials

Reactions were carried out in a pulsed-flow microcatalytic reactor connected to a dual-column gas chromatograph for the analysis of products (Fig. 1). The columns contained 13X molecular sieve and Porapak Q. Gases eluted from the GLC detector passed over a Geiger–Müller counter for measurement of radioactive (^{14}C) components. The reactor consisted of a cylindrical glass vessel fitted with a coarse glass sinter on which the catalyst (0.30 g) rested. The depth of the catalyst bed was typically 1 cm. Temperatures were measured by use of a thermocouple enclosed in a glass sheath located at the centre of the catalyst bed. The reactor was enclosed in a conventional furnace. Helium flowed through the reactor at a constant rate of 23 (cm^3 at STP) min^{-1}. Pulses of reactant gases (typically 3.6 cm^3 at 50–300 Torr) were introduced into this carrier

stream, and hence passed to the catalyst. The carrier gas then conveyed the products to the GLC and the radiocounting equipment (when required).

Titania-supported catalysts were examined in a static reactor (50 cm^3). Premixed reactants were admitted to the reactor, and samples extracted for analysis. Catalyst weights were again 0.30 g.

Compressed gases, H_2, CO, O_2, CO_2, C_2H_4, C_2H_6 (all >99.9%) were used as received. (There was no necessity to remove the last traces of air or oxygen from these materials because the catalysts used are not sensitive to poisoning by air (*3*).) $[^{14}C]C_2H_4$ (5 mCi $mmol^{-1}$) was diluted to the required activity per unit volume with $[^{12}C]C_2H_4$. [^{14}C]CO was prepared by the reduction of $[^{14}C]CO_2$ by metallic zinc at 675 K (*4*). [^{14}C]CO was diluted with a 1 : 3 mixture of $[^{12}C]CO_2$ and H_2, and $[^{14}C]CO_2$ was diluted with a 1 : 3 mixture of [^{12}C]CO and H_2. In each case the concentration of the radioactive component was 1000 ppm.

Activation energies quoted in Tables 2–4 are uncertain to ±4 kJ mol^{-1}.

RESULTS

The six cluster/support combinations, activated by heating to 523 K as described under Experimental Methods and in Part I (*1*), were immediately active for hydrogen isotope exchange and for ethene hydrogenation, ethane hydrogenolysis, CO hydrogenation, and CO_2 hydrogenation.

Hydrogen isotope exchange ($H_2 + D_2 \rightleftharpoons 2HD$) occurred too rapidly at 293 K for rate measurements to be made. Exchange was completely inhibited by the addition of just sufficient CO or ethene to saturate the available sites but was not noticeably reduced by the addition of a similar quantity of CO_2. This indicates that hydrogen, CO, and ethene compete for the same osmium atom sites on species A, CO and ethene being more strongly adsorbed than hydrogen, and that CO_2 is only weakly adsorbed, if at all, at these sites.

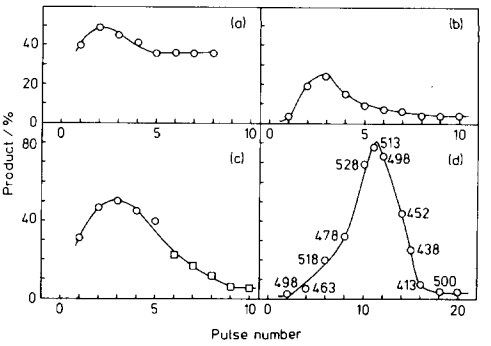

FIG. 2. Various manifestations of initial non-steady state behavior. (*a*) Ethene hydrogenation at 418 K ($C_2H_4 : H_2$ = 1 : 1) over species A derived from $Os_6(CO)_{18}$/silica; (*b*) CO hydrogenation to methane at 523 K ($CO : H_2$ = 1 : 3) over species A derived from $Os_3(CO)_{12}$/silica; (*c*) ethene hydrogenation at 418 K (circles) and CO hydrogenation at 625 K (squares) over species A derived from $Os_6(CO)_{18}$/silica; (*d*) ethane hydrogenolysis ($C_2H_6 : H_2$ = 1 : 1) at various specified temperatures over species A derived from $Os_3(CO)_{12}$/silica.

For each of the hydrogenations and ethane hydrogenolysis the initial activity shown by each catalyst was separated from the steady state activity that was finally achieved by a period of non-steady state behavior.

Non-Steady State Behavior

Figure 2 illustrates four examples of non-steady state behavior; each shows (i) a definite initial activity at pulse 1, (ii) a maximum in activity which is usually, though not necessarily, achieved at pulse 2 or 3, (iii) a region of declining activity, and (iv) the final attainment of reproducible activity at a level substantially lower than that achieved at the maximum. Figures 2*a* and *b* show this behavior for ethene hydrogenation at 418 K and for carbon monoxide hydrogenation at 523 K. Figure 2*c* shows that, when the maximum in the non-steady state for ethene hydrogenation was passed, a switch to CO hydrogenation at 625 K caused no perturbation and the activity continued to decline to a steady state value. A different behavior was observed when one reaction of such a pair was ethane hy-

TABLE 1

Hydrocarbon Retention during Non-Steady State Behavior

Catalyst[a]	Reaction[b]	Hydrocarbon retention [10^{18} C_2-units (g catalyst)$^{-1}$]		Site density (fresh catalyst) [10^{18} (g catalyst)$^{-1}$]
		At activity maximum	At the end of the non-steady state	
$Os_3(CO)_{12}$/alumina	$C_2H_4 + H_2 \rightarrow C_2H_6$	8.0	20.0	7.2
$Os_6(CO)_{18}$/silica	$C_2H_4 + H_2 \rightarrow C_2H_6$	5.0	8.5	6.6
$Os_3(CO)_{12}$/silica	$C_2H_6 + H_2 \rightarrow 2CH_4$	16.4	32.8	21.1

[a] Each catalyst is species A obtained by thermal activation of the stated cluster/support combination.
[b] $C_2H_4 : H_2 = 1:1$; $C_2H_6 : H_2 = 1:1$.

drogenolysis. For example, when a catalyst converted to the steady state by use of ethene hydrogenation was exposed to pulses of ethane and hydrogen, the observed hydrogenolysis activity passed through a further non-steady state cycle. The same effect was observed if the order of the reactions was reversed.

Figure 2*d* shows that similar non-steady state behavior was obtained even when temperature was varied considerably from one pulse to the next.

Product analyses during the non-steady state period showed a carbon imbalance in the sense that hydrocarbon was being progressively retained by the catalyst. Table 1 shows the extent of hydrocarbon retention at the maximum of the curve of rate against pulse number and at the point where the steady state was reached. The former is comparable with the chemisorption site density as monitored by the CO-adsorption capacities of the various species A (*2*).

Steady State Behavior

After passage through the non-steady state, catalysts showed reproducible activity over a sustained period, during which kinetic information was obtained. For each catalyst, conditions of flow rate and temperature were selected so as to achieve conversions mostly in the range 0.5 to 10%.

The information contained in Fig. 3 and Tables 2–4 was obtained from one set of catalysts; over each catalyst the reactions were investigated in the order: ethene hydrogenation, ethane hydrogenolysis, CO hydrogenation, CO_2 hydrogenation. Reaction rate, r, obeyed the usual equations $r = kP_1^m P_2^n$ and $k = A \exp(-E_{app}/RT)$ where P_1 represents the hydrocarbon pressure, P_2 the hydrogen pressure, and E_{app} the apparent activation energy. Thus the temperature-dependence of the rate was described by the equation

$$\log_{10} r_T = -E_{app}/2.303RT + C$$

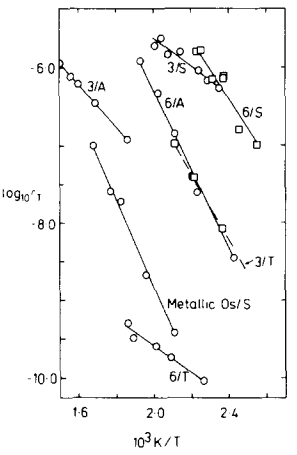

FIG. 3. Variation of rate with reciprocal temperature for ethane hydrogenolysis ($C_2H_6 : H_2 = 1:1$). (3/A) $Os_3(CO)_{12}$/alumina; (3/S) $Os_3(CO)_{12}$/silica; (3/T) $Os_3(CO)_{12}$/titania; (6/A) $Os_6(CO)_{18}$/alumina; (6/S) $Os_6(CO)_{18}$/silica; (6/T) $Os_6(CO)_{18}$/titania; (Metallic Os/S) conventional osmium/silica. The rate r has the units: mol s^{-1} (g catalyst)$^{-1}$.

where C is a constant. We were particularly concerned to establish whether activity patterns and activation energy sequences exhibited by this set of six catalysts were reproduced from one reaction to the next, and if so, whether these patterns and sequences could be related to the structural and chemisorption properties of species A as described in Parts I and II (*1, 2*).

Ethene hydrogenation. Catalysts were active at 325 K and above. Values of the orders of reaction and of the apparent activation energies are given in Table 2, together with those of $\log_{10}r$ for 390 K. Plots of $\log_{10}r_T$ against reciprocal temperature do not intersect in the range 325–535 K so the activity pattern for both $Os_3(CO)_{12}$- and $Os_6(CO)_{18}$-derived catalysts is that given in sequence (A):

Species A/silica > species A/titania
> species A/alumina Sequence (A)

The apparent activation energies are similar but the variation, such as it is, is in the opposite sense:

Species A/silica < species A/titania
< species A/alumina Sequence (B)

All apparent activation energies are higher than the value of 34 kJ mol^{-1} reported for ethene hydrogenation catalyzed by a conventional 2% osmium/alumina (*5*).

Ethane hydrogenolysis. Following the above investigation of ethene hydrogenation, the same catalysts were used to effect ethane hydrogenolysis. In each case, a further cycle of non-steady state behavior preceded steady state activity.

The variation of rate with reciprocal temperature is shown in Fig. 3; the figure also shows results obtained using a conventional 2% osmium/silica prepared by impregnation of $OsCl_3$ onto silica (Cab-O-Sil) from aqueous solution with subsequent reduction of the chloride to polycrystalline metal in hydrogen at 723 K.

All of the cluster-derived catalysts except that obtained from $Os_6(CO)_{18}$/titania were more active for methane formation than the conventional catalyst on the basis of the number of moles of ethane converted per unit weight of osmium present, and the apparent activation energies for reactions over the cluster-derived catalysts were all significantly lower than the value of 114 kJ mol^{-1} recorded for the conventional osmium/silica. For comparison, Sinfelt and Yates (*6*) report a value of 146 kJ mol^{-1} for 10% osmium/silica over the range 398–434 K. The apparent activation energies for the

TABLE 2

Kinetic Parameters for Ethene Hydrogenation[a]

Catalyst[b]	Order in ethene[c]	$\log_{10}r_{390}$[d]	Apparent activation energy (kJ mol^{-1})	Temperature range (K)
$Os_3(CO)_{12}$/alumina	0.1	−1.65	50	390–500
$Os_3(CO)_{12}$/silica	0.5	0.56	43	360–400
$Os_3(CO)_{12}$/titania	0.3	−0.15	44	355–390
$Os_6(CO)_{18}$/alumina	0.1	−1.52	48	490–535
$Os_6(CO)_{18}$/silica	1.0	−0.09	41	385–425
$Os_6(CO)_{18}$/titania	0.7	−0.54	45	325–425

[a] $C_2H_4 : H_2 = 1 : 1$.

[b] Each catalyst is species A obtained by thermal activation of the stated cluster/support combination.

[c] Order in hydrogen ≥ 1 except for $Os_6(CO)_{18}$/titania where the value was 0.2.

[d] Units of r: μmol s^{-1} (g catalyst)$^{-1}$.

TABLE 3

Kinetic Parameters for CO Conversion[a] to Methane and CO_2

Catalyst[b]	Methane formation		Carbon dioxide formation	
	E_a(kJ mol^{-1})	$\log_{10} r_{605}$[c]	E_a(kJ mol^{-1})	$\log_{10} r_{605}$[c]
$Os_3(CO)_{12}$/alumina	95 (540–645 K)	−3.21	97 (540–665 K)	−2.10
$Os_3(CO)_{12}$/silica	76 (455–665 K)	−0.48	39 (590–645 K)	0.20
$Os_3(CO)_{12}$/titania	93 (485–570 K)	−0.62	67 (485–570 K)	−1.35
$Os_6(CO)_{18}$/alumina	116 (570–665 K)	−3.69	23 (570–665 K)	−2.57
$Os_6(CO)_{18}$/silica	73 (590–665 K)	−0.32	[d]	[d]
$Os_6(CO)_{18}$/titania	80 (465–605 K)	−2.00	(465–605 K)	[e]

[a] $CO:H_2 = 1:3$.

[b] Each catalyst is species A obtained by thermal activation of the stated cluster/support combination.

[c] Units of r: μmol s^{-1} (g catalyst)$^{-1}$.

[d] Not measured.

[e] No detectable CO_2 formation (i.e., $\log_{10} r_{605} \leq -4.0$).

individual cluster-derived catalysts are $Os_3(CO)_{12}$/silica, 32 kJ mol^{-1} (425–500 K); $Os_3(CO)_{12}$/alumina, 52 kJ mol^{-1} (540–665 K); $Os_3(CO)_{12}$/titania, 81 kJ mol^{-1} (400–475 K); $Os_6(CO)_{18}$/silica, 75 kJ mol^{-1} (395–450 K); $Os_6(CO)_{18}$/alumina, 99 kJ mol^{-1} (410–515 K); $Os_6(CO)_{18}$/titania, 26 kJ mol^{-1} 450–535 K).

The pattern of activity for the various species A is complicated by multiple crossing of the lines shown in Fig. 3. However, for an average temperature of 473 K the activity pattern for $Os_3(CO)_{12}$-derived catalysts is that given by sequence (A) (above) in agreement with the situation for ethene hydrogenation. For the $Os_6(CO)_{18}$-derived catalysts this pattern is disturbed by the unexpectedly low activity of the species A derived from $Os_6(CO)_{18}$/titania. The apparent activation energies show no distinct patterns.

Carbon monoxide hydrogenation. Catalysts which had been used to examine ethene hydrogenation and ethane hydrogenolysis were then used for CO hydrogenation which occurred in a reproducible manner without any evidence of an initial non-steady state. Pulses of carbon monoxide and hydrogen in a 1:3 ratio were employed and the products were methane, carbon dioxide, and water, with traces of ethene and ethane. The kinetics of methane formation and of carbon dioxide formation are shown in Table 3. Straight-line plots of $\log_{10} r_T$ versus reciprocal temperature for methane formation over the six catalysts did not intersect over the range 455–665 K, and hence the listed values of $\log_{10} r_{605}$ provide the relative order of activities for any temperature within this range. The pattern of activity is again that given by sequence (A).

The pattern of activity for CO_2 formation over the $Os_3(CO)_{12}$-derived catalysts again conforms to sequence (A) because these plots of $\log_{10} r_T$ vs $1/T$ did not intersect.

The apparent activation energies for CO conversion (i) to methane over $Os_3(CO)_{12}$-derived catalysts, (ii) to methane over $Os_6(CO)_{18}$-derived catalysts, and (iii) to CO_2 over $Os_3(CO)_{12}$-derived catalysts in each case follow sequence (B).

Carbon dioxide hydrogenation. This reaction was the last of the four to be examined. Pulses of carbon dioxide and hydrogen in a 1:3 ratio reacted to give methane, carbon monoxide, and water as major products at temperatures for which kinetic in-

TABLE 4

Kinetic Parameters for CO_2 Conversion[a] to Methane and CO

Catalyst[b]	Methane formation		Carbon monoxide formation	
	E_a(kJ mol^{-1})	$\log_{10} r_{590}$[c]	E_a(kJ mol^{-1})	$\log_{10} r_{590}$[c]
$Os_3(CO)_{12}$/alumina	99 (525–625 K)	−2.34	118 (570–625 K)	−3.05
$Os_3(CO)_{12}$/silica	47 (540–625 K)	−0.20	97 (605–645 K)	−1.71
$Os_3(CO)_{12}$/titania	56 (455–590 K)	−0.40	(455–590 K)	[d]
$Os_6(CO)_{18}$/alumina	88 (570–690 K)	−2.78	105 (570–715 K)	−2.70
$Os_6(CO)_{18}$/silica	66 (570–665 K)	−0.82	98 (570–665 K)	−1.19
$Os_6(CO)_{18}$/titania	74 (475–605 K)	−2.34	68 (475–605 K)	−1.62

[a] $CO_2 : H_2 = 1 : 3$.

[b] Each catalyst is a species A obtained by thermal activation of the stated cluster/support combination.

[c] Units of r: μmol s^{-1} (g catalyst)$^{-1}$.

[d] No detectable CO formation (i.e., $\log_{10} r_{590} \leq -2.4$).

formation is given in Table 4. The activity pattern conforms to sequence (A) for (i) methane formation over $Os_3(CO)_{12}$-derived catalysts, (ii) methane formation over $Os_6(CO)_{18}$-derived catalysts, (iii) CO formation over $Os_6(CO)_{18}$-derived catalysts, and possibly for (iv) CO-formation over $Os_3(CO)_{12}$-derived catalysts.

Apparent activation energies for methane formation over $Os_3(CO)_{12}$- and $Os_6(CO)_{18}$-derived catalysts conform to sequence (B); however, the corresponding values for CO formation over $Os_6(CO)_{18}$-derived catalysts do not, and information for the $Os_3(CO)_{12}$-derived catalysts is incomplete.

Carbon Deposition in the Steady State

When catalysts showed reproducible activities, product analyses continued to show a carbon imbalance, i.e., hydrocarbon was still being progressively retained by the catalysts although the rate of retention was low. Apparent activation energies for the retention process that accompanied ethene hydrogenation were 38 kJ mol^{-1} over species A derived from $Os_3(CO)_{12}$/alumina (483–593 K); 40 kJ mol^{-1} over species A derived from $Os_3(CO)_{12}$/silica (364–440 K); 22 kJ mol^{-1} over species A derived from $Os_6(CO)_{18}$/silica (385–455 K).

Constitution and Reactivity of the Retained Hydrocarbon Species

The constitution of the retained species has been examined by infrared spectroscopy, and their reactivity by an isotope-exchange method.

A further fresh catalyst sample derived by thermal activation of $Os_3(CO)_{12}$/alumina was taken through the non-steady state to the steady state for ethene hydrogenation, and was then examined by infrared spectroscopy. Bands attributable to —CH_2— and —CH_3 groups were identified (blanks showed no bands) and the method of Yamasaki *et al.* (*7*) was used to quantify the numbers of such groups present by integration of band intensities. (This method does not detect —CH= or quarternary carbon.) Calculations indicated that 31×10^{18} methylene groups and 11×10^{18} methyl groups were present per gram of catalyst, and this should be compared with the presence of 7×10^{18} osmium atom adsorption sites per gram of catalyst determined from the measurement of a CO adsorption isotherm before use of the catalyst for ethene hydrogenation.

The retained hydrocarbon species were reactive; indeed, those formed during ethane hydrogenolysis were totally replaced

TABLE 5

Replacement of Retained Species Built up during Ethane Hydrogenolysis over $Os_6(CO)_{18}$/Silica in the Pulsed-Flow Reactor at ~425 K by Retained Species Derived from [^{14}C]Ethene Hydrogenation at ~415 K

Pulse No. ([^{14}C]C_2H_4 : H_2 = 1 : 1)	C_2-units retained/10^{17}		Total difference (10^{17} C_2-units)	Extent of replacement[a] (%)
	By GLC measurement	By measurement of ^{14}C count		
1	6	31	25	38
2	10	24	39	59
3	5	16	50	76
4	3	7	54	82
5	4	13	63	95
6	13	10	60	91
7	2	2	60	91

[a] Total C_2-units retained during ethane hydrogenolysis at 425 K before the first pulse of (ethene + hydrogen)-mixture = 66×10^{17}.

by ethene when the test reaction was switched to ethene hydrogenation. This was demonstrated as follows. A further fresh catalyst sample derived from $Os_6(CO)_{18}$/silica was first taken through the non-steady state to the steady state for ethane hydrogenolysis, and then used to hydrogenate ethene containing [^{14}C]C_2H_4. The catalyst showed non-steady state behavior over the course of the next seven reactions, all of which are recorded in Table 5. In the first, 52% of the radioactivity in the sample was lost to the catalyst whereas GLC analysis showed a loss of C_2-material of only 11%. This disparity lessened with each succeeding experiment until the losses concurred at pulse 7. The extent to which the total material loss as measured by radiochemical analysis exceeded the loss as measured by gas chromatography amounted to 19×10^{18} C_2-units (g catalyst)$^{-1}$, and this compared with the initial presence of 21×10^{18} C_2-units (g catalyst)$^{-1}$ on the catalyst at the end of the non-steady state for ethane hydrogenolysis.

Isotope Tracer Studies of CO and CO_2 Hydrogenations

Methane formed in CO hydrogenation may be a primary product or a secondary product formed by CO_2 hydrogenation. To judge between these alternatives, (CO + $3H_2$)-mixtures containing 1000 ppm [^{14}C]CO_2 were passed over three catalysts and the products analyzed radiochemically and by GLC. [^{14}C]CO_2 was adsorbed under these conditions, as shown by its reduction to [^{14}C]CO, but it was not hydrogenated to [^{14}C]CH_4 (Table 6). Consequently, [^{12}C]CH_4 formed simultaneously was a primary product of [^{12}C]CO hydrogenation, not a secondary product via [^{12}C]CO_2 hydrogenation.

The apparent activation energies for the reduction of [^{14}C]CO_2 to [^{14}C]CO (see Table 6) were 66 kJ mol^{-1} over the range 488–573 K for reactions over the catalyst derived from $Os_3(CO)_{12}$/titania and 84 kJ mol^{-1} over the range 543–648 K for reactions over the catalyst derived from $Os_6(CO)_{18}$/alumina. These values are each uncertain to ±12 kJ mol^{-1} (uncertainties of this magnitude are inherent in the radiochemical experiment). Comparison with the apparent activation energies listed in Tables 3 and 4 shows that these values are comparable with those for CO_2 hydrogenation to methane and are substantially lower than those for CO hydrogenation to methane.

It was also important to determine whether CO was a true intermediate in the hydrogenation of CO_2 to methane. For this

TABLE 6

Products of the Hydrogenation[a] of a ($^{12}CO + H_2$)-Mixture Containing 1000 ppm $^{14}CO_2$ (Reaction 1) and of a ($^{12}CO_2 + H_2$)-Mixture Containing 1000 ppm ^{14}CO (Reaction 2)

Reaction	Catalyst[b]	Temp (K)	Stable products (%)			Labelled products (%)		
			^{12}CO	$^{12}CO_2$	$^{12}CH_4$	^{14}CO	$^{14}CO_2$	$^{14}CH_4$
1	$Os_3(CO)_{12}$/alumina	560	94.5	5.0	0.5	4.5	95.5	0.0
1	$Os_3(CO)_{12}$/titania	500	94.6	2.1	3.3	11.8	88.2	0.0
		560	56.8	8.9	34.3	15.3	84.7	0.0
1	$Os_6(CO)_{18}$/alumina	570	96.3	3.6	0.1	2.0	98.0	0.0
2	$Os_3(CO)_{12}$/alumina	570	0.9	94.2	4.9	0.0	29.2	70.8
2	$Os_6(CO)_{18}$/alumina	645	7.0	83.6	9.4	0.0	24.4	75.6

[a] $^{12}CO : H_2 = 1:3$; $^{12}CO_2 : H_2 = 1:3$.

[b] Each catalyst is species A obtained by thermal activation of the stated cluster/support combination.

purpose ($CO_2 + 3H_2$)-mixtures containing 1000 ppm [^{14}C]CO were passed over the same two catalysts and the products analyzed. All [^{14}C]CO was rapidly removed from the reaction mixture under conditions where [^{12}C]CO was being formed from [^{12}C]CO_2 in measurable yields. This result is interpreted in the Discussion.

DISCUSSION

The rate of a catalyzed reaction depends upon the concentrations of the species that participate in the rate-determining step, and these concentrations are usually determined by the nature of the adsorption sites and by competition of reactants for these sites. To understand the behavior of these cluster-derived catalysts, it is important to appreciate that the nature and properties of the sites they contain differ significantly from those at the surface of crystalline osmium.

The formulae presented for species A in the Experimental Methods section indicate that, given a nuclearity for species A of about 12, an average cluster may chemisorb one to five CO molecules. Adsorption is severely restricted in this way because of the large number of CO-ligands bonded to each cluster (24–34) and because some osmium atoms are involved in the support–cluster interaction. Thus, for example, for species A derived from $Os_6(CO)_{18}$/silica, only exceptional osmium atoms have the residual bonding capacity to act as adsorption sites for CO, and even these will be bonded to several osmium neighbors and to CO-ligands. We are therefore concerned with catalytic activity at sites which may be isolated and which are sterically congested. Consequently, the situation is very different from that at the surface of an osmium crystallite where we can expect osmium atom sites to be surrounded by equivalent neighbors in the surface.

The Non-Steady State

The non-steady state was characterized by a progressive loss of hydrocarbon throughout, during which activity rose, passed through a maximum, and then declined (Fig. 2). The retained hydrocarbon during the subsequent steady state was reactive (in that it could be replaced by an alternative reacting hydrocarbon, Table 5) and contained both methyl and methylene groups. This replaceability of retained hydrocarbon indicates that it is formed and remains at the osmium atom sites of species A. In the steady state, hydrocarbon loss to the catalyst continued at a slow rate, but activity was unaffected (see below).

We interpret these findings for the situation involving ethene hydrogenation, but

the model is applicable, *mutatis mutandis,* to the other reactions.

The initial activity observed in the first reaction over a freshly prepared catalyst (Fig. 2*a*) represents the nearest approach that can be made to an activity measurement in the absence of retained hydrocarbon. Ethene molecules were adsorbed at the vacant sites (which have been demonstrated to be present by CO and O_2 adsorption measurements (*2*)) and reacted with hydrogen which adsorbed in competition. This represents the inherent activity of species A.

The first trend in the non-steady state was that activity increased; this occurred despite the fact that hydrocarbon was progressively retained so that the concentration of sites for ethene adsorption and reaction decreased. We infer from this that the retained hydrocarbon acted as a hydrogen transfer agent and that the effective concentration of adsorbed hydrogen was thereby increased. Thomson and Webb (*8*) have claimed for some years that hydrocarbon retained at the conventional metal catalyst surface plays an active and sometimes all-important role in hydrogen transfer to adsorbed hydrocarbons; we propose that analogous processes occur in reactions catalyzed by our various species A. Such retained hydrocarbonaceous material can only transfer a hydrogen atom to ethene adsorbed in the immediate vicinity. Thus, bearing in mind the localized nature of the sites present on species A, we propose that pairs of osmium atoms (which act as sites for CO or O_2 adsorption (*2*)) may accommodate one retained hydrocarbonaceous species and one ethene molecule. Ethene hydrogenation is envisaged to occur as shown in Scheme 1, where the retained hydrocarbon is represented as R—CH_x—M or as R—CH_{x-1}—M, the bond from carbon to the osmium atom site, M, being single or multiple depending on the value of x. The rise in activity noted in the non-steady state indicates that hydrogen atom acquisition by the retained hydrocarbon species and its subsequent transfer to adsorbed-C_2H_4 and -C_2H_5 (steps 2, 3, 4, and 5) is a faster process than the direct acquisition of adsorbed hydrogen atoms from the osmium atom sites (steps 6 and 7).

The maximum activity in the non-steady state was soon achieved (Fig. 2) and further hydrocarbon retention led to a decline in activity. This may have occurred because both sites of the pair symbolized in Scheme 1 became occupied by retained hydrocarbon, and neither was then available for ethene adsorption. Alternatively, the retained hydrocarbon represented as R—CH_x—M or R—CH_{x-1}—M may have homologated to R′—CH_x—M or R′—CH_{x-1}—M which then provided increased steric inhibition of ethene adsorption at the second site of the pair. Probably

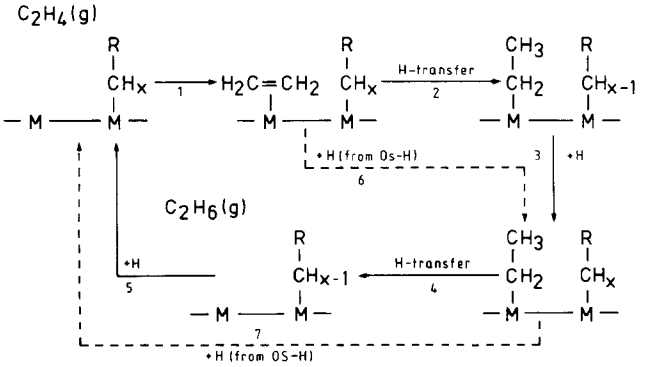

SCHEME 1. Ethene hydrogenation facilitated by hydrogen atom transfer from retained hydrocarbon species.

both processes contributed. The deactivation continued until the steady state was reached, at which point activity was normally at least an order of magnitude lower than that achieved at the maximum. In the steady state, progressive hydrocarbon loss did not affect activity, from which we conclude that homologation had proceeded to the point where further lengthening of the hydrocarbon chain did not effectively increase steric inhibition at ethene adsorption sites. The likelihood remains, however, that the retained hydrocarbon was the principal vehicle of hydrogen atom transfer to adsorbed-C_2H_4 and -C_2H_5 over catalysts in the steady state.

The retained hydrocarbon species contained methyl and methylene groups as shown by infrared spectroscopy. The total extent of carbon loss measured by GLC exceeded by a factor of 2 or 3 the carbon content as represented by the species accounted for by infrared spectroscopy. The balance presumably represents carbon present as —CH= and as quaternary carbon. This suggests that the retained hydrocarbon on catalysts in the steady state was branched-chain in structure and unsaturated in character.

This model also interprets the non-steady state behavior observed in the hydrogenation of CO and of CO_2 and in the hydrogenolysis of ethane. In the hydrogenation of the carbon oxides to methane, adsorbed-CH and adsorbed-CH_2 are important intermediates, and these also participate in chain-lengthening processes (*9–12*). We propose that these processes give comparable retained hydrocarbon species. It is therefore no surprise that once a catalyst was taken through the non-steady state to the steady state for any one of the hydrogenations, it immediately provided steady state behavior for any of the others. Remarkably, however, catalysts in the steady state for hydrogenations exhibited a fresh non-steady state when used for ethane hydrogenolysis (and vice versa). We conclude that the site environment required for ethane hydrogenolysis differed from that required for hydrogenation.

Support Effects on Steady State Activity

The steady state activities of our catalysts for each of the three hydrogenations and for ethane hydrogenolysis (the latter within a restricted temperature range) followed the pattern represented by sequence (A), viz:

Species A/silica > species A/titania
> species A/alumina

The difference in activity between species A/silica and species A/alumina was 1½–2 orders of magnitude for ethene hydrogenation (Table 2) and ethane hydrogenolysis (Fig. 3) and 2–3 orders of magnitude for CO and CO_2 hydrogenations (Tables 3 and 4).

The site densities of the various fresh catalysts, as measured by CO and O_2 chemisorptions, varied at most by one-half of an order of magnitude (see Experimental Methods and Table 1). Hence the pattern of steady state activity is not directly related to the initial site densities of the catalysts.

The conversion of catalysts from the freshly prepared state to the steady state was accompanied by considerable hydrocarbon retention (Table 1) and hence the observed activity pattern may, in principle, be a synthesis of three factors, (i) an effect of the extent of hydrocarbon retention on site density, (ii) a steric effect of retained hydrocarbon on site activity, and (iii) a direct support effect on site activity. These factors are not likely to be independent because a direct effect of the support on site activity for hydrogenation or hydrogenolysis may also manifest itself as a support effect on the polymerization process that constitutes hydrocarbon retention; thus factor (iii) may predetermine factors (i) and (ii). We therefore seek an interpretation of sequence (A) in the general area of support effects.

In Part I we established that species A contains some osmium atoms in the zero oxidation state and some in formal oxida-

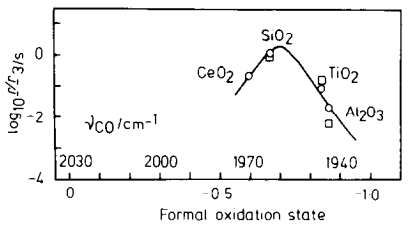

FIG. 4. Variation of activity, r, with the frequency ν of CO (in cm^{-1}) bonded to the atoms of species A in a partially negative formal oxidation state. Activities are expressed relative to the value for species A derived from $Os_3(CO)_{12}$/silica, $r_{3/S}$. (○) Catalysts derived from $Os_3(CO)_{12}$; (□) catalysts derived from $Os_6(CO)_{18}$.

tion states that are either partially negative or partially positive (*1*). We noted that the frequency of the infrared absorption band for ligand-CO bonded to osmium in the partially negative oxidation state depended upon the support employed, and proposed that the band position provided a measure of the support–cluster interaction. Figure 4 shows the manner in which the logarithm of the steady state activity for ethene hydrogenation varies with the extent of the support–cluster interaction as measured by the frequency of this absorption band for silica-, titania-, and alumina-supported catalysts. Clearly, activity declines as the support–cluster interaction is developed. Graphs comparable with Fig. 4 were obtained for the other three reactions.

In 1973 Primet *et al.* (*13*) demonstrated that the frequency of the absorption band of CO adsorbed on platinum was sensitive to the co-adsorption of electron-withdrawing entities (e.g., Cl) or electron-donating entities (e.g., pyridine). Electron donors increased backdonation from platinum to anti-bonding orbitals on carbon, thus strengthening the Pt–C bond, weakening the C–O bond, and decreasing ν_{CO}. Electron-withdrawing species had the opposite effect. In our catalysts, osmium atoms of species A which act as ethene adsorption sites are also bonded to ligand-CO. Thus, electron displacements which affect the Os–C–O system will also influence Os–C_2H_4, so that ν_{CO} provides information on the adsorbent–adsorbate interaction. On the assumption that ethene is chemisorbed as a π-complex, we argue as follows. An increase in electron donation from the support to species A increases backdonation both from osmium to ligand-CO and from (the same) osmium to adsorbed-C_2H_4, with the effect that ν_{CO} is decreased and ethene becomes more strongly chemisorbed. Figure 4 is then interpreted to mean that, as we pass from silica to titania to alumina, so the support–cluster interaction increases, the adsorbed species become more strongly adsorbed, and activity is diminished.

The portion of the curve in Fig. 4 containing the points for silica, titania, and alumina, should constitute one side of a "volcano" plot, and the question arises as to where the maximum is located. We require for comparison a support which gives a species A having $\nu_{CO} > 1965$ cm^{-1} for ligand-CO bonded to osmium in a partially negative formal oxidation state. We have been fortunate to find that a catalyst prepared by impregnation of $Os_3(CO)_{12}$ onto ceria and activated by our standard procedure gave species A having the empirical formula $Os_n(CO)_{3.0n}C_{0.2n}Z_{0.0(2)n}$ and for which the appropriate ν_{CO} was located at 1970 cm^{-1}. The activity of this material for ethene hydrogenation is also shown in Fig. 4. The position of species A/ceria on Fig. 4 suggests that we are indeed dealing with a volcano relationship, and that the maximum is occupied by species A/silica. Further evidence for such a relationship will be presented in Reference (*14*) which is concerned with variously supported species A derived from $H_4Os_4(CO)_{12}$.

The activity of species A/ceria was intermediate between that of species A/silica and species A/titania not only for ethene hydrogenation, but also for ethane hydrogenolysis and CO_2 hydrogenation. CO hydrogenation was not examined.

Reaction Mechanisms

Ethene hydrogenation. Cluster-derived materials catalyzed ethene hydrogenation

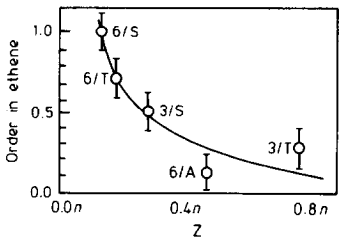

FIG. 5. Ethene hydrogenation. Variation of the order of reaction in ethene with site concentration, Z, in species A determined by CO chemisorption (see Experimental Methods for values and definition of Z). (3/S) $Os_3(CO)_{12}$/silica; (6/T) $Os_6(CO)_{18}$/titania, etc.

only at temperatures well above room temperature; the reaction exhibited orders in ethene which were fractionally positive and apparent activation energies were in the range 41–50 kJ mol^{-1} (Table 2). These characteristics differ from those provided by metallic osmium for which activity was considerable even at 273 K, the order in ethene was zero, and the apparent activation energy 34 kJ mol^{-1} (*5, 15*). The positive orders in ethene suggest that ethene adsorption on the cluster-derived catalysts was weak, and in consequence, higher temperatures were required to obtain measurable product formation from low steady-state concentrations of adsorbed-C_2H_4. This conclusion is supported by an inverse dependence of the order in ethene on the site concentration in species A which embraces all catalysts except $Os_3(CO)_{12}$/alumina (Fig. 5). A greater commitment of species A to bonding with ligand-CO leads to weaker ethene adsorption, and the weaker the adsorption the more positive is the reaction order in ethene.

Ethane hydrogenolysis. Ethane hydrogenolysis over osmium/silica has been studied by Sinfelt and Yates (*6*), who inferred that ethane dissociates at the metal surface to give adsorbed-C_2 and that the rate determining step is carbon–carbon bond rupture. This implies that the site must involve a considerable number of metal atoms, since six hydrogen atoms have to be accommodated in the adsorbed state, as well as the highly unsaturated C_2-entity. Other authors have been more specific in their statements concerning site demands in ethane hydrogenolysis; for example, Martin (*16*) has suggested that 12 adjacent metal atoms are required in order to achieve the dissociative adsorption of ethane on nickel/silica. The cluster size of species A and the highly restricted nature of the sites present necessitate a somewhat different mechanism for ethane hydrogenolysis over the cluster-derived catalysts.

The cluster-derived catalysts (except $Os_6(CO)_{18}$/titania) were more active, per unit weight of osmium present, than metallic osmium supported on silica (Fig. 3). The same is true if activity is measured in terms of the turnover number, N, at 500 K. For species A derived from $Os_3(CO)_{12}$/silica, N/molecules $site^{-1}$ s^{-1} = 7.5×10^{-3} for the catalyst at the commencement of the non-steady state, 1.2×10^{-1} at the maximum in the non-steady state, and 6.8×10^{-2} in the steady state; this compares with a value of 1.5×10^{-4} for osmium/silica behaving in a reproducible state. (These values have been calculated by use of site concentrations estimated from CO adsorption isotherms for catalysts in the *freshly prepared* state; this has been necessary in view of uncertainties that would be implicit, in principle, in the interpretation of CO isotherms for these catalysts in the used state. Since site concentrations for species A diminish during the non-steady state (see above), the true values exceed those quoted.)

A detailed discussion of mechanism must await more detailed kinetic studies. However, it is reasonable to suppose that the number and nature of the osmium atom sites in species A restrict the extent of dissociation of ethane, and that carbon–carbon bond rupture occurs in adsorbed-C_2H_x where x is unknown, but may be 3, 4, or 5 as in ethane hydrogenolysis over metallic Ru or Co (*17–19*). This implies a weaker adsorption of ethane on species A than on metallic osmium, which accords with the substantially lower apparent activation en-

ergies afforded by the cluster-derived catalysts by comparison with the values reported by Sinfelt and co-workers and by ourselves for metallic osmium supported on silica.

Carbon monoxide hydrogenation. There are no detailed reports of osmium-catalyzed CO hydrogenation in the literature. However, recent work in this laboratory has shown that conventional 2% osmium/silica, 2% osmium/alumina, and 2% osmium/titania exhibit activities, per unit weight of osmium present, which are similar to those of species A derived from $Os_3(CO)_{12}$/silica and $Os_6(CO)_{18}$/silica. The apparent activation energies for reaction over these three conventional catalysts were 110, 119, and 112 kJ mol^{-1}, respectively, which is similar to that reported here for species A derived from $Os_6(CO)_{18}$/alumina (Table 3).

The appearance of CO_2 as a primary product during CO hydrogenation to methane was not unexpected (*20, 21*). However, since the formation of methane from CO_2 was often faster than from CO (Tables 3 and 4) it was necessary to establish whether or not secondary hydrogenation of CO_2 to methane occurred during CO hydrogenation. Reaction 1 in Table 6 shows that $[^{14}C]CO_2$ introduced into CO hydrogenation was adsorbed and reduced to $[^{14}C]CO$ but not hydrogenated to $[^{14}C]CH_4$. Secondary processes were therefore absent in reactions described in Table 3.

Carbon produced in the Boudouard reaction ($2CO \rightarrow CO_2 + C$) over conventional metals is an active intermediate in CO hydrogenation for the formation of methane and higher hydrocarbons (*9–11*). The same reaction is also responsible for the presence of ligand-C in species A (see Part I).

A general scheme for CO hydrogenation is shown in Scheme 2; in our reactions higher hydrocarbon yields were negligible. The rate-determining step for methane formation is probably located in the sequence of steps 3–6, because orders in hydrogen were positive for methane formation and zero for CO_2 formation. Furthermore, when a catalyst in the steady state for CO hydrogenation was exposed to pulses of pure hydrogen the formation of methane continued. In this case the C_1-intermediate concerned in the rate-determining step of CO conversion to methane remained adsorbed after passage of the $(CO + H_2)$-pulse and was removable by subsequent H_2-pulses. In part A of Table 7 the rates of methane formation are compared (i) during CO hydrogenation, (ii) during the removal of the C_1-intermediate by the H_2-pulse; values for (ii) have been calculated on the assumption that the C_1-intermediate was (*a*)

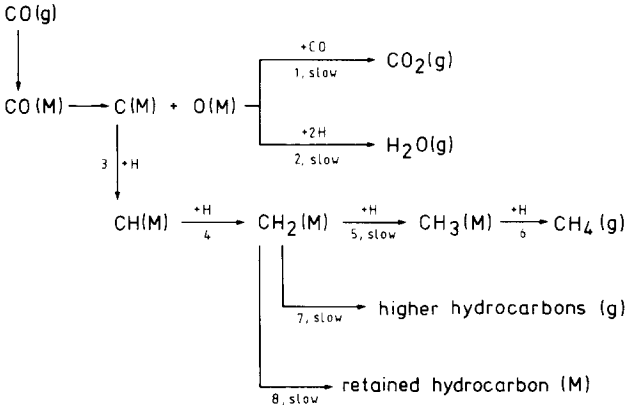

SCHEME 2. Proposed mechanism for CO hydrogenation; (M) denotes the adsorption of an intermediate at an osmium atom site of species A.

TABLE 7

Rates of Methane Formation, r, Measured over $Os_3(CO)_{12}$/Silica in the Pulsed-Flow Reactor during CO Hydrogenation and CO_2 Hydrogenation, and during the Passage of Hydrogen Pulses after each of these Reactions

Pulse composition	$\log_{10} r_{523}$[a]				
	Catalyst in steady state	Calculated for $CH_x(ads) + \frac{(4-x)}{2}H_2 \rightarrow CH_4(g)$			
		$x = 0$	$x = 1$	$x = 2$	$x = 3$
A {CO : H_2 = 1 : 3	−0.73				
A {Pure H_2		−0.44	−0.57	−0.75	−1.05
B {CO_2 : H_2 = 1 : 4	−0.35				
B {Pure H_2		−0.36	−0.49	−0.67	−0.96

[a] Units of r μmol s^{-1} (g catalyst)$^{-1}$; temperature = 523 K.

C(ads); (*b*) CH(ads); (*c*) CH_2(ads); (*d*) CH_3(ads). The rates concur for the case in which the C_1-intermediate is CH_2(ads), and we thus propose step (5) as the rate-determining step.

Adsorbed-CH_2 is often regarded as the intermediate that initiates carbon–carbon bond formation (*11*), and hence the production of retained hydrocarbon and gaseous higher hydrocarbons. In the present work the rate of formation of retained hydrocarbon was of negative order in hydrogen, whereas methane formation, as noted above, was of positive order. These observations are consistent with the removal of adsorbed-CH_2 by steps (5), (7), and (8) of Scheme 2.

We envisage that the retained hydrocarbon acts as an efficient hydrogen transfer agent, and that this is the main source of hydrogen for steps (2)–(6) in Scheme 2.

Carbon dioxide hydrogenation. Attempts to measure isotherms for CO_2 adsorption at 293 K by the method described in Part II failed and we conclude that CO_2, unlike CO and O_2, does not chemisorb to a measurable extent at this temperature at the osmium atom sites of species A. A similar conclusion was drawn above from the observations that CO inhibited hydrogen isotope exchange on species A at 293 K whereas CO_2 did not. The situation at the elevated temperatures used for CO_2 hydrogenation where CO is a product is complex.

The tracer experiments described in Table 6 show two important features. First, in Reaction 1 the conversion of $[^{14}C]CO_2$ to $[^{14}C]CO$ occurred in the presence of a large excess of $[^{12}C]CO$. This demonstrates (i) the dissociative adsorption of CO_2:

$$CO_2(g) \rightarrow CO(ads) + O(ads) \qquad (1)$$

and (ii) the existence of a distinct site for CO_2 adsorption since the osmium sites of species A were occupied by strongly adsorbed CO under these conditions. Second, in Reaction 2, the low concentration of $[^{14}C]CO$ was completely converted to $[^{14}C]CO_2$ and $[^{14}C]CH_4$ in the presence of a large excess of $[^{12}C]CO_2$ and H_2. This is understandable if the $[^{14}C]CO_2$ was adsorbed at sites other than the osmium atoms of species A, in which case the $[^{14}C]CO$ was free to adsorb at the osmium sites along with a great excess of hydrogen whereupon rapid hydrogenation occurred.

Thus, at reaction temperatures (455–690 K), CO_2 adsorbs at a location on species A other than the osmium atom sites.

The rate-determining step for methane

formation was determined by a method analogous to that described above for CO hydrogenation. The rate of methane formation in CO_2 hydrogenation over $Os_3(CO)_{12}$/silica at 523 K was determined by passing (CO_2 + H_2)-pulses over the catalyst in the usual way, and the rate compared with that subsequently observed when the strongly held C_1-intermediate left behind was removed by a pulse of pure hydrogen. Part B of Table 7 shows that the rates concur when the intermediate is assumed to be adsorbed-C.

The following mechanism accommodates these observations ((*) represents the adsorption site which initially accommodates CO_2 and (M) represents an osmium atom adsorption site of the type active in CO hydrogenation.) In Equation (7) x = 1 or 2.

$$CO_2(g) \longrightarrow CO(*) + O(*) \quad (1)$$

$$CO(*) \xrightarrow[\text{slow}]{} CO(g) \quad (2)$$

$$CO(*) \longrightarrow C(*) + O(*) \quad (3)$$

$$C(*) \xrightarrow[\text{slow}]{+H} CH(*) \quad (4)$$

$$CH(*) \xrightarrow[\text{fast}]{+H} CH_2(*) \xrightarrow[\text{fast}]{+H} CH_3(*) \xrightarrow[\text{fast}]{+H} CH_4 \quad (5)$$

$$O(*) \xrightarrow[\text{slow}]{+2H} H_2O(g) \quad (6)$$

$$CH_x(*) \longrightarrow CH_x(M) \xrightarrow{+(2-x)H} CH_2(M) \xrightarrow{\text{slow}} \text{retained hydrocarbon} \quad (7)$$

The special site for CO_2 adsorption on species A is likely to be carbonaceous in character. When CO_2 is hydrogenated over a freshly prepared catalyst the only alternative to osmium as a site for CO_2 adsorption is ligand-C. Species A in a steady state catalyst possesses also retained hydrocarbon, some of which may resemble ligand-C in its general properties. Ligand-C was shown in Part II (*2*) to function as a site for the weak adsorption of CO at 293 K. Further evidence concerning the site for CO_2 adsorption must await the measurement of CO_2 adsorption isotherms at elevated temperatures.

The hydrogen atoms involved in steps (4), (5), and (6) may be supplied by transfer from the retained hydrocarbon (compare Scheme 1) or by migration from osmium atom sites. The role of the retained hydrocarbon as a hydrogen transfer agent may be less dominant in CO_2 hydrogenation than in the other reactions reported here, because hydrogen molecules can adsorb at the osmium atom sites without competition and hence a relatively high surface coverage of adsorbed hydrogen atoms is to be expected.

Migration of intermediates from ligand-C sites to osmium sites cannot contribute to the initial methane formation because of the presence of a second kinetically slow step, viz: $CH_2(M) \xrightarrow{+H} CH_3(M)$ (see CO hydrogenation, above). However, methane could be formed by this route after an induction period, and Step (7) provides a route for the continued accumulation of retained hydrocarbon in reactions taken to high conversion.

Finally, we recall that the apparent activation energy for the conversion of $[^{14}C]CO_2$ to $[^{14}C]CO$ in the context of CO hydrogenation over $Os_6(CO)_{18}$/alumina was 84 kJ mol^{-1} (above, text) whereas the value for the conversion of CO_2 to CO during CO_2 hydrogenation over the same catalyst was 105 kJ mol^{-1} (Table 4). We suspect the latter value to be misleading in the sense that, at low temperatures where CO yields were low, a substantial proportion of the CO formed in Step (2) may have been lost to the initial product by readsorption at osmium atom sites from which it was released later in the reaction as methane. At high temperatures, where CO yields were high, such losses would have been inconsequential. Thus, 84 kJ mol^{-1} is probably the more secure value of the apparent activation energy for the conversion of CO_2 to CO over $Os_6(CO)_{18}$/alumina. The values for this process quoted in Table 4 for other catalysts should, similarly, be treated with caution.

ACKNOWLEDGMENTS

This work was part of a Joint Research Scheme funded by Imperial Chemical Industries and carried out at the University of Hull. We thank Dr. D. Urwin of Tioxide Limited for a gift of pure titania.

REFERENCES

1. Collier, G., Hunt, D. J., Jackson, S. D., Moyes, R. B., Pickering, I. A., Wells, P. B., Simpson, A. F., and Whyman, R., *J. Catal.* **80,** 154 (1983).
2. Hunt, D. J., Jackson, S. D., Moyes, R. B., Wells, P. B., and Whyman, R., *J. Catal.* **86,** 333 (1984).
3. Hunt, D. J., Jackson, S. D., Moyes, R. B., Wells, P. B., and Whyman, R., *J. Chem. Soc. Chem. Commun.* 85 (1982).
4. Bernstein, R. B., and Taylor, T. I., *Science* **21,** 498 (1947).
5. Bond, G. C., Webb, G., and Wells, P. B., *Trans. Faraday Soc.* **61,** 999 (1965).
6. Sinfelt, J. H., and Yates, D. J. C., *J. Catal.* **10,** 362 (1968).
7. Yamasaki, H., Kobori, Y., Naito, S., Onishi, T., and Tamaru, K., *J. Chem. Soc. Faraday I* **77,** 2913 (1981).
8. Thomson, S. J., and Webb, G., *J. Chem. Soc. Chem. Commun.* 526 (1976); Al-Ammar, A. S. and Webb, G., *J. Chem. Soc. Faraday I* **74,** 195 (1978); Webb, G., *in* "Catalysis" (C. Kemball and D. A. Dowden, Eds.), Vol. 2, pp. 145–175. Chemical Society, London, 1978.
9. Wentrcek, P. R., Wood, B. J., and Wise, H., *J. Catal.* **43,** 363 (1976).
10. Rabo, J. A., Risch, A. P., and Poutsma, M. L., *J. Catal.* **53,** 295 (1978).
11. Biloen, P., Helle, J. N., and Sachtler, W. M. H., *J. Catal.* **58** 95 (1979).
12. Denny, P. J., and Whan, D. A., *in* "Catalysis" (C. Kemball and D. A. Dowden, Eds.), Vol. 2. pp. 46–86. Chemical Society, London, 1978.
13. Primet, M., Basset, J. M., Mathieu, M. V., and Prettre, M., *J. Catal.* **29,** 213 (1973).
14. Hunt, D. J., Jackson, S. D., Moyes, R. B., Wells, P. B., and Whyman, R., accepted for presentation at the Eighth International Congress on Catalysis, Berlin, 1984.
15. Webb, G., Ph.D. thesis, University of Hull, 1963.
16. Martin, G. A., *J. Catal.* **60,** 345 (1979).
17. Sinfelt, J. H., *Catal. Rev.* **3,** 175 (1970).
18. Sinfelt, J. H., and Yates, D. J. C., *J. Catal.* **8,** 82 (1967).
19. Sinfelt, J. H., Taylor, W. F., and Yates, D. J. C., *J. Phys. Chem.* **69,** 95 (1965).
20. Araki, M., and Ponec, V., *J. Catal.* **44,** 439 (1976).
21. Sachtler, J. W. A., Kool, J. M., and Ponec, V., *J. Catal.* **56,** 284 (1979).